Cellulose (2020) 27:6383–6398
https://doi.org/10.1007/s10570-020-03241-3

ORIGINAL RESEARCH

Durable and recyclable Ag/AgCl/CeO_2 coated cotton fabrics with enhanced visible light photocatalytic performance for degradation of dyes

Xinmei Guan · Yifei Zhan · Lin Yang · Jianwu Lan · Jiaojiao Shang · Siqi Chen · Wenxu Li · Shaojian Lin

Received: 27 December 2019 / Accepted: 14 May 2020 / Published online: 25 May 2020

Abstract In this work, a highly efficient and recyclable composite photocatalyst was successfully prepared via grafting Ag/AgCl/CeO_2 on the surface of cotton fabric. First of all, the amino functionalized Ag/AgCl/CeO_2 with the optimum composition was prepared. Then, the amino functionalized Ag/AgCl/CeO_2 nanoparticles were grafted on the aldehyde functionalized cotton fabrics via "amine–aldehyde" chemistry reaction to obtain targeted composite photocatalysts. The surface microstructure and chemical composition of the resultant cotton fabric (Ag/AgCl/CeO_2–CF) were characterized by FT-IR, XPS and SEM, respectively. The results showed that the Ag/AgCl/CeO_2 nanoparticles have been successfully grafted onto the cotton fabric surface. Moreover, the grafted amount of Ag/AgCl/CeO_2 on the surface of cotton fabric can be regulated by the aldehyde functionalized degree of cotton fabric. As expected, the photocatalytic experiments demonstrated that the Ag/AgCl/CeO_2 decorated cotton fabric exhibited excellent photocatalytic activity. It could degrade 99.5% of MB, 95.2% of RhB and 92.6% of MO within 180 min under visible light irradiation, respectively. Most importantly, the degradation efficiency could still maintain 80.7% after five degradation cycles, suggesting that the Ag/AgCl/CeO_2–CF possessed outstanding reusable performance without centrifugation and filtration.

Xinmei Guan and Yifei Zhan have contributed equally to this work.

Electronic supplementary material The online version of this article (https://doi.org/10.1007/s10570-020-03241-3) contains supplementary material, which is available to authorized users.

X. Guan · Y. Zhan · L. Yang · J. Lan (✉) · J. Shang · S. Chen · W. Li · S. Lin (✉)
College of Biomass Science and Engineering, Sichuan University, Chengdu 610065, China
e-mail: lanjw@scu.edu.cn

S. Lin
e-mail: sjlin@scu.edu.cn

Graphic abstract

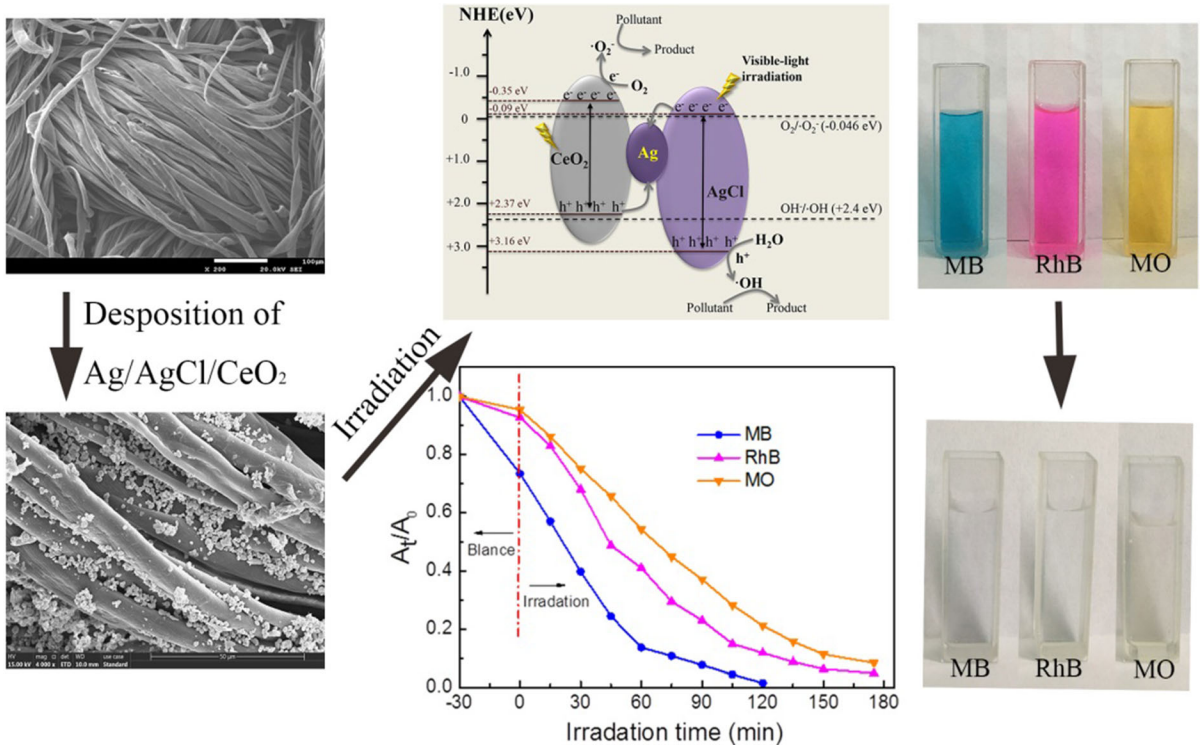

Keywords $Ag/AgCl/CeO_2$ · Cotton fabric · Photocatalytic degradation · Recyclability

Introduction

With the rapid economic growth, the industrial waste water containing various synthetic dyes has attracted considerable attention, due to serious threat to human health and ecological environment (Fu et al. 2019; Cheng et al. 2016; Li et al. 2014; Peng et al. 2018). As a promising method to address this issue, semiconductor-based photocatalytic oxidation technology has a hopeful application prospect in wastewater treatment owing to its environmental friendly, energy saving, mild reaction conditions and without secondary contamination (Fu et al. 2019; Dong et al. 2019; Li et al. 2019a, b; Monti et al. 2016; Wu et al. 2016; Yadav and Purkait 2016; Yang et al. 2015; Yi et al. 2019). In the past decades, in order to take full use of solar light, numerous scientists have devoted to explore various semiconductor photocatalysts with visible light photocatalytic activity for degradation of various synthetic dyes, such as g-C_3N_4, Ag/AgCl, Bi_2WO_6 and V_2O_3 (Qin et al. 2019; Gashti et al. 2012; Montazer and Pakdel 2011; Shekofteh-Gohari et al. 2018; Zinatloo-Ajabshir and Salavati-Niasari 2016; Ouyang et al. 2018).

Among of all them, Ag/AgX (Cl, Br and I) have attracted considerable attention recently, due to prominent capability of harvesting solar energy in a very broad visible spectrum (Bi and Ye 2009). This outstanding visible light photocatalytic performance of Ag/AgX can be ascribed to, besides the surface plasmon resonance (SPR) effect of Ag nanoparticles, the highly dispersed AgX species. AgX can improve the separation efficiency of photo-generated charge carriers and generate electron–hole pairs when they absorb photos, resulting in enhanced photocatalytic activity of the substrates (Jiang and Zhang 2011; Liu et al. 2017). This is the reason that Ag/AgX exhibits better visible light photocatalytic activity than that of Ag nanoparticles. Nevertheless, the photocatalytic activity of Ag/AgX is limited by its photocorrosion during the continuous visible light photocatalytic

process (Zhang et al. 2014), which seriously hinders their photocatalytic stability. Fortunately, numerous investigations showed that silver halides can maintain their stability and photocatalytic activity with the assistance of other semiconductor materials (TiO_2, SiO_2 and ZnO etc.) to promote the transfer of the photo-excited carriers (Shekofteh-Gohari et al. 2018; Sun et al. 2014). For example, Zang and Farnood synthesized a catalyst by doping AgBr on TiO_2 that can efficiently degrade MO under visible light irradiation, following the significant improvement of stability of AgBr during photocatalytic process (Zang and Farnood 2008). Yu et al. prepared a durable AgI–TiO_2/PAN catalyst, which showed a highly photocatalytic activity in degradation of MO. Moreover, the degradation efficiency of MO over AgI–TiO_2/PAN was much higher as compared to that of pure PAN, AgI/PAN and TiO_2/PAN, due to the synergistic effect between AgI and TiO_2 (Yu et al. 2016). Noteworthily, preparation of heterostructures via incorporating two or more semiconductor materials has been demonstrated as one of the best choices to enhance photocatalytic activity resulting from the synergistic effects between different semiconductors. Recently, ceric dioxide (CeO_2) as a relatively inexpensive rare earth semiconductor has been widely utilized to fabricate heterostructure photocatalysts (Lin et al. 2015; Kaviyarasu et al. 2016; Sangsefidi et al. 2017). Inspiration from these investigations, introduction of CeO_2 into Ag/AgX to improve its stability and photocatalytic activity is highly desirable. More importantly, CeO_2 can couple well with Ag/AgX due to their matched band structures (Wen et al. 2017). Based on this reason, Zeng et al. firstly prepared Ag/AgCl–CeO_2 composite photocatalysts with 5.12 to 17.76 wt% Ag/AgCl for the photodegradation of norfloxacin (NOF) under visible light irradiation (Wen et al. 2017). However, the photocatalytic efficiencies of reported Ag/AgCl/CeO_2 were still quite low. As mentioned in the literature, the AgX content had a strong effect in their photocatalytic activity (Yu et al. 2016). Inspiration from this result, we introduced a little amount of CeO_2 into Ag/AgCl to prepared novel Ag/AgCl/CeO_2. Herein, CeO_2 plays a role in facilitating the transfer of photogenerated electrons and improving the stability of Ag/AgCl, resulting in the novel Ag/AgCl/CeO_2 composite materials with higher photocatalytic activity and structural stability under visible light irradiation.

Apart from photocatalytic activity, photocatalysts with facile and durable reusability are also essential for practical application. It is well known that the photocatalyst powder may reduce its photocatalytic activity seriously after aggregation in practical applications. Moreover, the powdery catalyst is not conducive to recycling, which may cause secondary contamination and potential cytotoxic effects (Du et al. 2018). To address these drawbacks, such photocatalyst powders usually were anchored on the surfaces of substrates (Ran et al. 2019; Wang et al. 2017; Tissera et al. 2015). Among all of them, cotton fabric was frequently employed as the substrate to immobilize nanoparticles, due to its various characteristics including good mechanical properties, large specific surface area, porosity, controllable structure, and biodegradability (Guan et al. 2019; Li et al. 2008; Rafatullah et al. 2010; Ran et al. 2019; Zhan et al. 2019). Moreover, cotton fabric is easily modified owing to existence of abundant active moieties. In our previous work, the Ag/AgCl/ZIF-8/TiO_2 coated cotton fabric was successfully prepared for highly efficient phtocatalytic degradation of dyes under visible light irradiation (Guan et al. 2019). This functional cotton fabric can be easily reused to photocatalyze dye degradation without centrifugation or filtration. However, the Ag/AgCl/ZIF-8/TiO_2 easily detached from cotton fabric during photocatalytic process. Therefore, another objective of this work is to realize steady interfacial adhesion between Ag/AgX/CeO_2 and cotton fabrics to form efficient and durable photocatalysts for dye degradation.

In the current work, an Ag/AgCl/CeO_2 decorated cotton fabric with high visible light photocatalytic activity and easy reusability was successfully developed (Scheme 1). First, Ag/AgCl/CeO_2 composites are prepared via a facile co-precipitation method, and then the surface was modified with amino groups via utilization of (3-aminopropyl) triethoxysilane (ATPMS) as a coupling agent. Subsequently, such amino-functionalized Ag/AgCl/CeO_2 nanoparticles are grafted on the aldehyde functionalized cotton fabric via "amine–aldehyde" chemistry reaction. The surface microstructure and composition of resultant cotton fabric are characterized by FT-IR, SEM, EDS and XPS measurements. Secondly, the photocatalytic performance of Ag/AgCl/CeO_2 decorated cotton fabric is evaluated via degradation of methylene blue (MB), rhodamine B (RhB) and methyl orange (MO)

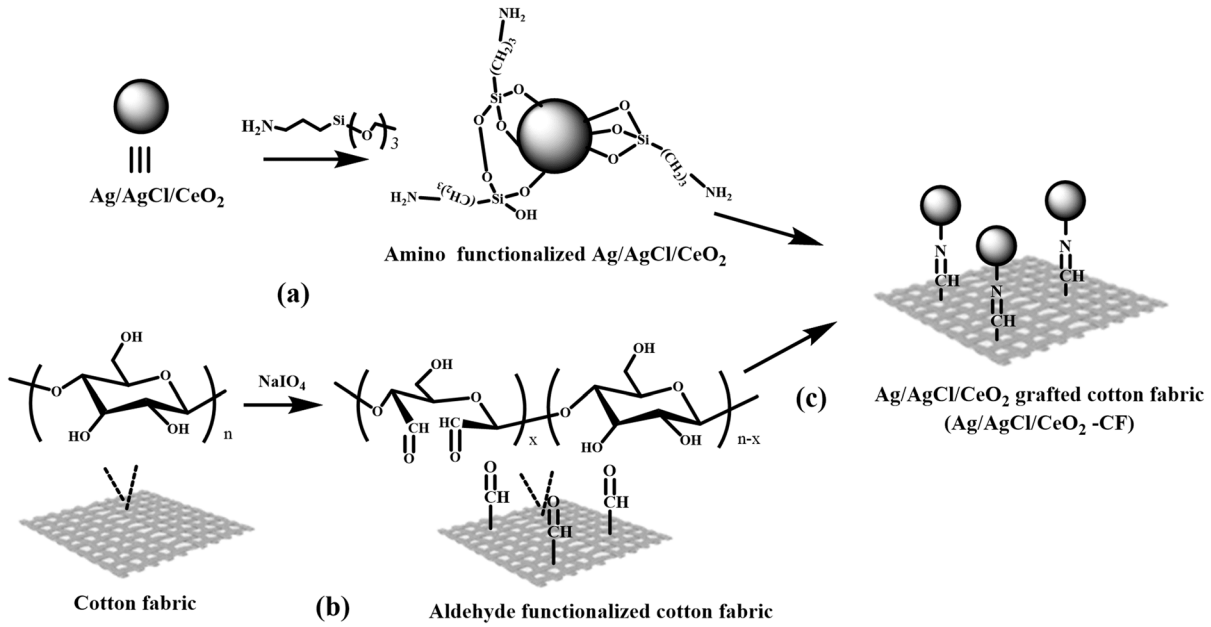

Scheme 1 Illustration of the fabricated route of $Ag/AgCl/CeO_2$ grafted cotton fabrics as highly efficient photocatalysts

under visible light irradiation. Finally, the recyclability and the possible mechanism of $Ag/AgCl/CeO_2$ decorated cotton fabric towards various dyes are also investigated in detail.

Experimental

Materials

Cotton fabric (CF) with plain weave structure was purchased from a local fabric store. Methylene blue (MB, 98.5%), rhodamine B (RhB), methyl orange (MO), ceric dioxide (CeO_2, 99%), sodium periodate ($NaIO_4$, 99.5%), silver nitrate ($AgNO_3$, 99.0%), zinc chloride ($ZnCl_2$, 98%), ethanol (CH_3CH_2OH, 99.7%), ethylene glycol ($(CH_2OH)_2$, 99.5%), tert-butylacohol ($C_4H_{10}O$, 99.0%), ethylenediamine tetra acetic acid disodium salt ($C_{10}H_{14}N_2Na_2O_8$, 98.0%), *p*-benzoquinone ($C_6H_4O_2$, 98.0%), (3-aminopropyl) triethoxysilane (ATPMS) were bought from China Kelon Chemical Reagent Co., Ltd without further purification before used.

Preparation of photocatalysts

Preparation of Ag/AgCl/CeO₂

0.374 g of $AgNO_3$ was dissolved in 40 mL of deionized water, and then a certain proportion of CeO_2 (3 wt%, 7 wt%, 10 wt%, 13 wt% and 16 wt%) was added to the solution under magnetic stirring for 30 min. Next, 0.13 g $ZnCl_2$ was added into the suspending solution and the mixture was stirred for 30 min. Then, the suspension was irradiated by a xenon lamp for 30 min with stirring to achieve the photoreduction. Subsequently, the suspension was filtered and washed three times with deionized water and dried at 60 °C for 2 h to obtain the $Ag/AgCl/CeO_2$ nanoparticles with different CeO_2 weight ratios of 3%, 5%, 7%, 10%, 13%, and 16%, denoted as $Ag/AgCl/CeO_2$ (3 wt%), $Ag/AgCl/CeO_2$ (5 wt%), $Ag/AgCl/CeO_2$ (7 wt%), $Ag/AgCl/CeO_2$ (10 wt%) and $Ag/AgCl/CeO_2$ (16 wt%), respectively, for further procedure.

Amino functionalized Ag/AgCl/CeO₂

Herein, amino functional $Ag/AgCl/CeO_2$ was prepared (Scheme 1a). First, a certain amount of coupling agent (ATPMS) was dissolved into ethanol/DI water

mixture (v:v = 85:15) to form 5 wt% solution. Then, 2 g of Ag/AgCl/CeO_2 was added with magnetic stirring for 2 h at room temperature. Finally, the suspension was filtered and washed three times with excess deionized water to remove residual ATPMS and dried at 60 °C in vacuum oven to obtain the surface amino functionalized Ag/AgCl/CeO_2 nanoparticles with varying CeO_2 contents.

Preparation of aldehyde functionalized cotton fabric

Cotton fabric (4 cm × 4 cm) was immersed in 100 mL of sodium periodate solution with various concentrations (0.01 g mL^{-1}, 0.03 g mL^{-1}, 0.05 g mL^{-1}, 0.07 g mL^{-1} and 0.10 g mL^{-1}) at 50 °C for 4 h under dark conditions, respectively (Scheme 1b). Subsequently, the aldehyde functionalized cotton fabric was soaked in 0.1% (w/w) ethylene glycol solution with stirring for 30 min at room temperature. Finally, the resultant cotton fabric was washed and dried. According to the increment of concentration of $NaIO_4$, the aldehyde functionalized cotton fabrics were labeled as CF-1, CF-2, CF-3, CF-4 and CF-5, respectively.

Preparation of Ag/AgCl/CeO_2 decorated cotton fabric

0.25 g amino functionalized Ag/AgCl/CeO_2 nanoparticles were dispersed in 100 mL of deionized water at 50 °C, then aldehyde functionalized cotton fabrics were immersed into solution for 2 h to realize Ag/AgCl/CeO_2 graft on the surface of cotton fabric via "amine–aldehyde" chemistry reaction (Scheme 1c). Subsequently, the resultant samples were washed by deionized water for three times, and then dried at 60 °C for 24 h for following experiments. According to the degree of aldehyde of cotton fabric, the Ag/AgCl/CeO_2 grafted cotton fabrics were named as Ag/AgCl/CeO_2–CF1, Ag/AgCl/CeO_2–CF2, Ag/AgCl/CeO_2–CF3, Ag/AgCl/CeO_2–CF4 and Ag/AgCl/CeO_2–CF5, respectively. Herein, Ag/AgCl/CeO_2 coated untreated cotton fabric was also prepared for comparison according to the same procedure, and denoted as Ag/AgCl/CeO_2–CF0.

Characterization

FT-IR spectra of the samples were measured with a Nicolet 560 Fourier transform infrared spectrophotometer (USA) in the wavenumber ranging from 600 to 4000 cm^{-1}, the fabric samples were measured by ATR accessory. X-ray photoelectron spectroscopy (XPS) measurements were performed on a Kratos XSAM800 system with an Al Ka (hv = 1486.6 eV) 150 W, the shift in binding energy caused by the relative surface charge is calibrated with reference to the peak of C 1s. The surface morphologies of the samples were recorded on a JEOL JSM-7500F Field Emission Scanning Electron Microscope (SEM). The UV–visible spectroscopy of the samples was carried out on a UV-2700 spectrophotometer (Shimadzu) in the range of 200–800 nm. The light absorption properties of the samples were recorded using a UV–Vis spectrophotometer. The electrochemical impedance spectroscopy measurement (EIS) was carried out on electrochemical workstation (Instrument Model: CHI660E) with the frequency range from 100 kHz to 0.01 Hz and the amplitude of 5 mV. The counter and the reference electrodes were platinum wire and saturated calomel electrode (SCE), respectively, and the electrolyte solution was phosphate buffer saline.

Photocatalytic activity

The photocatalytic activity of the prepared samples were carried out by photocatalytic degradation of dyes under visible light irradiation ($\lambda > 420$ nm) of a 500 W xenon lamp (GXZ500, Shanghai, China). The distance between the light source and the sample is 25 cm. The resultant coated sample was immersed in a 50 mL solution having a concentration of 20 mg L^{-1}. Subsequently, the solution was stored in the dark for 30 min to achieve an adsorption–desorption equilibrium. During the irradiation time, 3 mL of the degradation solution was taken out and the absorbance of the solution was measured at intervals of 15 min, and then poured back into the degradation solution after the test. The absorbance ratio of the solution (A_t/A_0) was used to measure the photodegradation efficiency of the prepared sample. A_0 is the initial absorbance of the degradation liquid, A_t is the absorbance of the degradation liquid in reaction time t after being irradiated.

In addition, the photocatalytic stability and recyclability of Ag/AgCl/CeO_2–CF were also investigated. The photocatalytic mechanism was studied by different scavenger capture experiments in order to detect

potential active species involved in the degradation process.

Results and discussion

Photocatalytic activity of Ag/AgCl/CeO_2

First of all, a series of Ag/AgCl/CeO_2 nanoparticles were prepared. Their structures were confirmed by SEM and XPS, respectively. The corresponding results were presented in Figs. S1 and S2. The results confirmed that the Ag/AgCl/CeO_2 heterostructures were successfully prepared. Then, the photocatalytic performances of the as-prepared samples with various compositions were investigated via the photodegradation of MB experiment under visible light irradiation. As shown in the UV–Vis spectra of all powder samples (Fig. 1a), it is obvious that introduction of CeO_2 into Ag/AgCl can effectively improve light absorption range and intensity from 400 to 800 nm. As expected, the photocatalytic activities of Ag/AgCl/CeO_2 heterostructures were better than both of pure Ag/AgCl and CeO_2 (Fig. 1b). However, the photocatalytic activity of Ag/AgCl/CeO_2 decreased after the amount of CeO_2 exceeded 10 wt%. This result may be ascribable to the aggregation of CeO_2 particles, and thus results in a shading effect (Jiang et al. 2019). As shown in Fig. 1b, the Ag/AgCl/CeO_2(10%) exhibited the best photocatalytic activity, which can be attributed to the good synergistic effect between Ag/AgCl and CeO_2, resulting in enhanced separation efficiency of photogenerated electron–hole pairs. For this reason, the Ag/AgCl/CeO_2(10%) was utilized in following experiments. Moreover, as shown in Fig. 1c, Ag/AgCl/CeO_2(10%) could degrade almost MB, RhB and MO within 15 min, further suggesting that Ag/AgCl/CeO_2(10%) could be considered as an effective photocatalyst.

Characterization of Ag/AgCl/CeO_2 decorated cotton fabrics

Herein, the FT-IR, XPS and SEM were employed to confirm the structures of Ag/AgCl/CeO_2 decorated cotton fabrics (Ag/AgCl/CeO_2–CF). First of all, the successful fabrication of Ag/AgCl/CeO_2–CF based on "amine–aldehyde" chemistry reaction was confirmed by FT-IR measurement. Taking Ag/AgCl/CeO_2–CF5 as an example, the corresponding results were presented in Fig. 2. Compared to pristine cotton fabric, besides the characteristic absorption bands at 3300 cm^{-1}, at 2897 cm^{-1} and at 1027–1060 cm^{-1} from cellulose could be observed (Chen et al. 2019), it is obvious that the oxidization of cotton fabric by $NaIO_4$ created aldehyde groups on its surface, which could be indicated by the appearance of characteristic peak at 1740 cm^{-1} for the stretching vibration of C=O of the aldehyde group (Wan et al. 2017; Zhao et al. 2015) (Fig. 2b). Further, the aldehyde functionlized cotton fabrics reacted with amino functionalized Ag/AgCl/CeO_2, resulting in the characteristic adsorption bands at 1740 cm^{-1} disappeared and a new characteristic adsorption band peak of –Si–O–C– could be found at 1021 cm^{-1} on cotton fabric (Wen et al. 2019), which belonged to the amino functionalized Ag/AgCl/CeO_2 (Fig. S3). Based on above mentioned results, it demonstrated that amino functionalized Ag/AgCl/CeO_2 nanoparticles have been successfully grafted on the surface of cotton fabric via formation of Schiff base structure.

In order to further confirm the composition of resultant cotton fabric, the XPS measurement was performed. The survey XPS spectrum of Ag/AgCl/CeO_2–CF5 was displayed in Fig. 3a, the results showed that the presence of C, N, O, Si, Ag and Cl elements in the as-prepared sample, proved that amino functionalized Ag/AgCl/CeO_2 nanoparticles have been successfully loaded onto the cotton fabric via "amino-aldehyde" chemistry reaction. Noteworthily, the peak of Ce was not observed in the Fig. 3a due to the weak signal of Ce. Additionally, the high-resolution narrow spectrum of the main characteristic elements C, O, Ag, Si and N were presented in Fig. 3b–f, respectively. The C1s was showed in Fig. 3b, deconvolution of the C1s spectrum could give several peaks, the peaks at 284.6 eV, 286.6 eV, 288.1 eV could be attributed to C–C, C–O, and C=O bond from cotton fabric, respectively. The composition C–Si (283.5 eV), C–N (285.5 eV), C–OH (288.1 eV) bond mainly resulted from ATPMS (Li et al. 2019a, b; Wan et al. 2017; Wen et al. 2019). And the C=N species suggested the chemical reaction between cotton fabric and Ag/AgCl/CeO_2, which was consistent with the results from FT-IR. The XPS spectrum of O1s was also fitted, as shown in Fig. 3c, the three

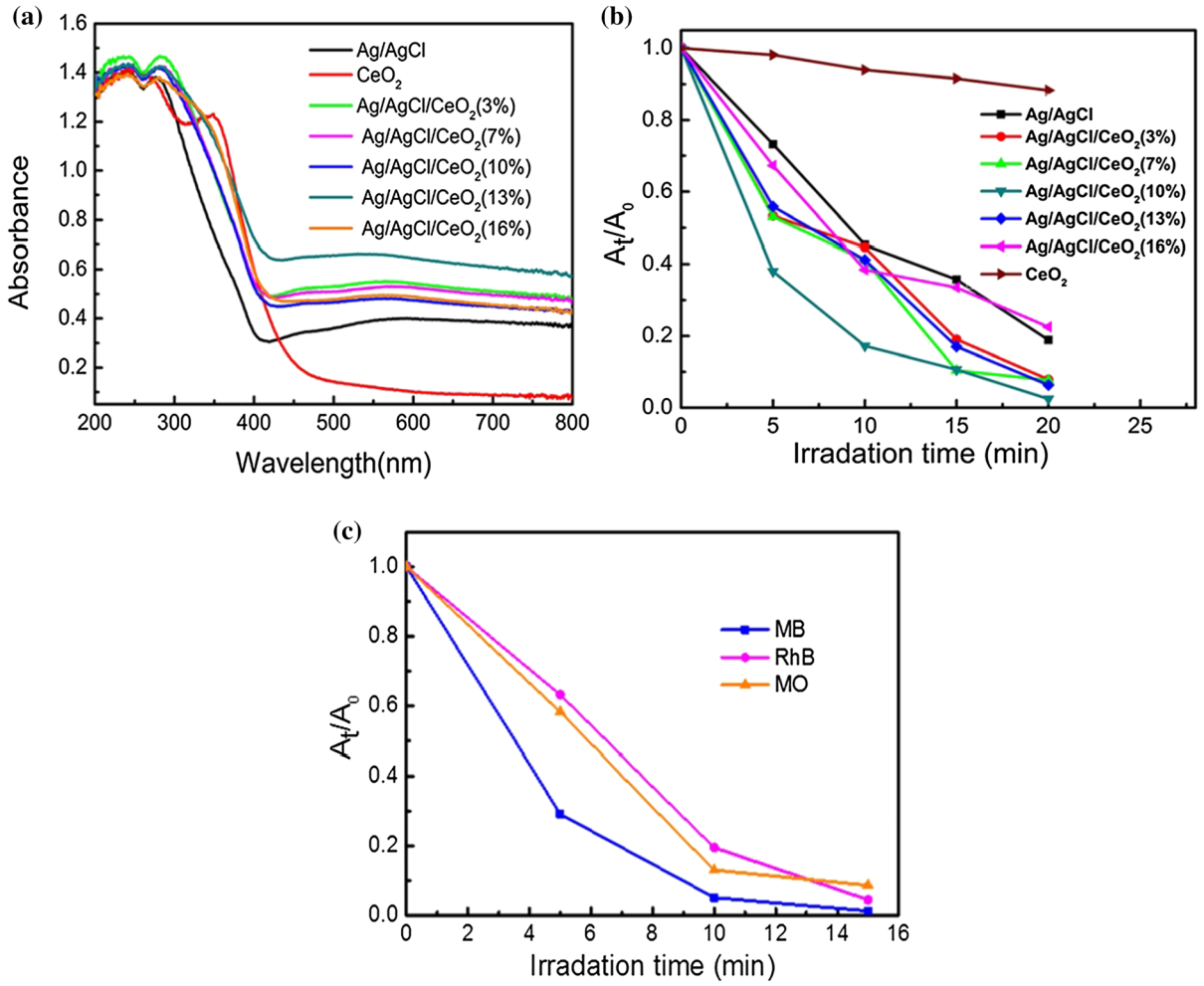

Fig. 1 **a** UV–Vis diffuse reflectance spectra of as-prepared samples, **b** photocatalytic degradation of MB by different samples under visible-light irradiation, **c** photocatalytic degradation of MB, RhB and MO by Ag/AgCl/CeO_2(10%)

fitting peaks at 533.1 eV, 535.3 eV, 531.9 eV could be attributed to C–O, C=O or Si–OH and Si–O–Si, which could also verify that ATPMS existed on the fabric. Ag 3d was displayed in Fig. 3d, the peaks at 373.7 eV and 367.8 eV could be attributed to the Ag^0 species, the peaks at 373.1 eV and 367.2 eV could be ascribed to the Ag^+ species, proved the presence of Ag/AgCl (He et al. 2017; Yao and Liu 2014). Meanwhile, as shown in Fig. 3e, the peaks at 101.4 eV, 102.3 eV, 103.1 eV are the binding energy of Si–O–Si, Si–O–H and Si–O–C, respectively (Li et al. 2008). The N and Si element could both attribute in amino functionalized Ag/AgCl/CeO_2, indicating that the Ag/AgCl/CeO_2 nanoparticles were successfully grafted on the cotton fabric surface.

After FT-IR and XPS measurements, the SEM test was employed to visualize the microstructure of prepared Ag/AgCl/CeO_2–CF. The surface morphologies of samples were presented in Fig. 4. It was showed that the pristine cotton fabric was smooth with few pits and grooves (see Fig. 4a). However, the nanoparticles can be obviously observed on Ag/AgCl/CeO_2–CF (Fig. 4b–f). Moreover, the amount of Ag/AgCl/CeO_2 increased with increment of aldehyde degree of cotton fabric. This result further demonstrated that Ag/AgCl/CeO_2 loaded on the surfaces of cotton fabrics based on "amine–aldehyde" chemistry reaction. It is good agreement with the results from FT-IR measurement. In addition, utilization of Ag/

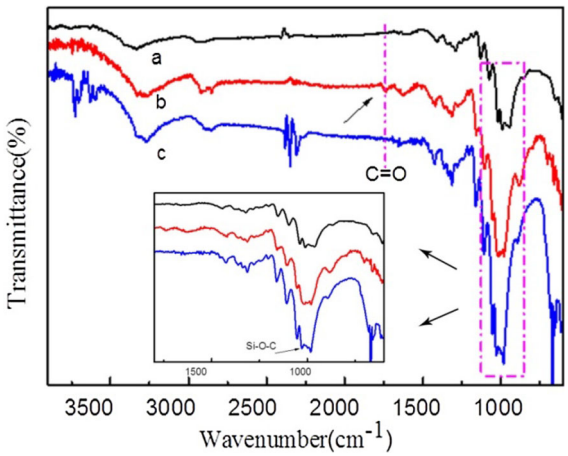

Fig. 2 FTIR spectra of **a** pristine cotton fabric, **b** aldehyde functionalized cotton fabric and **c** Ag/AgCl/CeO_2 decorated cotton fabric

AgCl/CeO_2–CF5 as an example, the EDS analysis was conducted. The results indicated that existence of Ag, O, Si, N, Cl and Ce elements in the resultant sample (Fig. 4g). Meanwhile, a detail chemical analysis was performed using element mapping, as shown in Fig. 4h–l, it can be clearly seen that the distribution of the Ag element is consistent with the Cl. Moreover, the Si and Ce elements were distributed on the entire surface, indicating that Ag/AgCl/CeO_2 had been grafted on the cotton fabric. Until now, it can be concluded from the results of FT-IR, XPS and SEM measurements that the targeted Ag/AgCl/CeO_2–CFs has been successfully prepared.

UV–Vis data analysis

In order to better understand photocatalytic behavior, the optical absorption property was also investigated by UV–Vis diffuse reflectance spectra in order to verify whether the functionalized cotton fabric can absorb visible light. As shown in Fig. 5a, no absorption peaks can be observed from the pristine cotton fabric in the range from 200 to 800 nm, indicating that it has no ultraviolet-visible absorption capacity. Nevertheless, after grafting Ag/AgCl/CeO_2 on the surface of cotton fabric, its absorption capacity in the range from 200 to 400 nm was significantly improved. Based on the results from UV–Vis spectra, the band gap of different materials can be calculated by the formula (Tauc 1974): $(Ahv) = K(hv - Eg)^{\frac{n}{2}}$. Where A, h, v, K and E_g represent the absorption coefficient, Planck's constant, incident light frequency, a constant and the band-gap energy, respectively. Taking Ag/AgCl/CeO_2–CF5 as an example, Fig. 4b shows the bandgaps of different composites by plotting $(Ahv)^2$ versus hv. The Egs of Ag/AgCl and CeO_2 from Ag/AgCl/CeO_2–CF5 were 2.83 eV and 3.75 eV, respectively, these results are similar with the data from the previous report (Wen et al. 2017).

Photocatalytic activity of Ag/AgCl/CeO_2 decorated cotton fabrics

After successful preparation of Ag/AgCl/CeO_2–CFs, their photocatalytic activities were investigated in detail. First, the photocatalytic activity of cotton fabric with different amounts of Ag/AgCl/CeO_2 was studied. As shown in Fig. 6, all samples exhibited satisfactory visible light photocatalytic performance. As expected, the Ag/AgCl/CeO_2–CF5 presented the highest degradation efficiency among all of them (Fig. 6a). This result can be ascribed to the possession of most of the photocatalyst on the surface of the cotton fabric by Ag/AgCl/CeO_2–CF5, resulting in excellent photocatalytic capacity. Herein, EIS was also utilized to evaluate the electrochemical performance of photocatalysts. The corresponding results were shown in Fig. 6b. The arc radius represents the electron transfer efficiency. It is well known that the smaller radius indicates a better the electron transfer rate. The arc radius of Ag/AgCl/CeO_2–CF5 was smaller than other samples, implying that it has better photocatalytic performance due to the faster electron transfer rate than that of others (Qi et al. 2019), suggesting that more Ag/AgCl/CeO_2 had loaded on the cotton fabric surface, which was consistent with the SEM results.

Based on above mentioned results, the Ag/AgCl/CeO_2–CF5 was employed in further experiments due to its outstanding photocatalytic activity. For the purpose of evaluating the photocatalytic property of Ag/AgCl/CeO_2–CF5 catalysts, MB, RhB and MO were selected as contaminants. As shown in Fig. 6c, the Ag/AgCl/CeO_2–CF5 showed excellent degradation efficiency for all dyes. The degradation efficiencies of MB, RhB and MO were 99.5%, 95.2% and 92.6%, respectively, under visible light irradiation for 180 min. This result indicated that the Ag/AgCl/

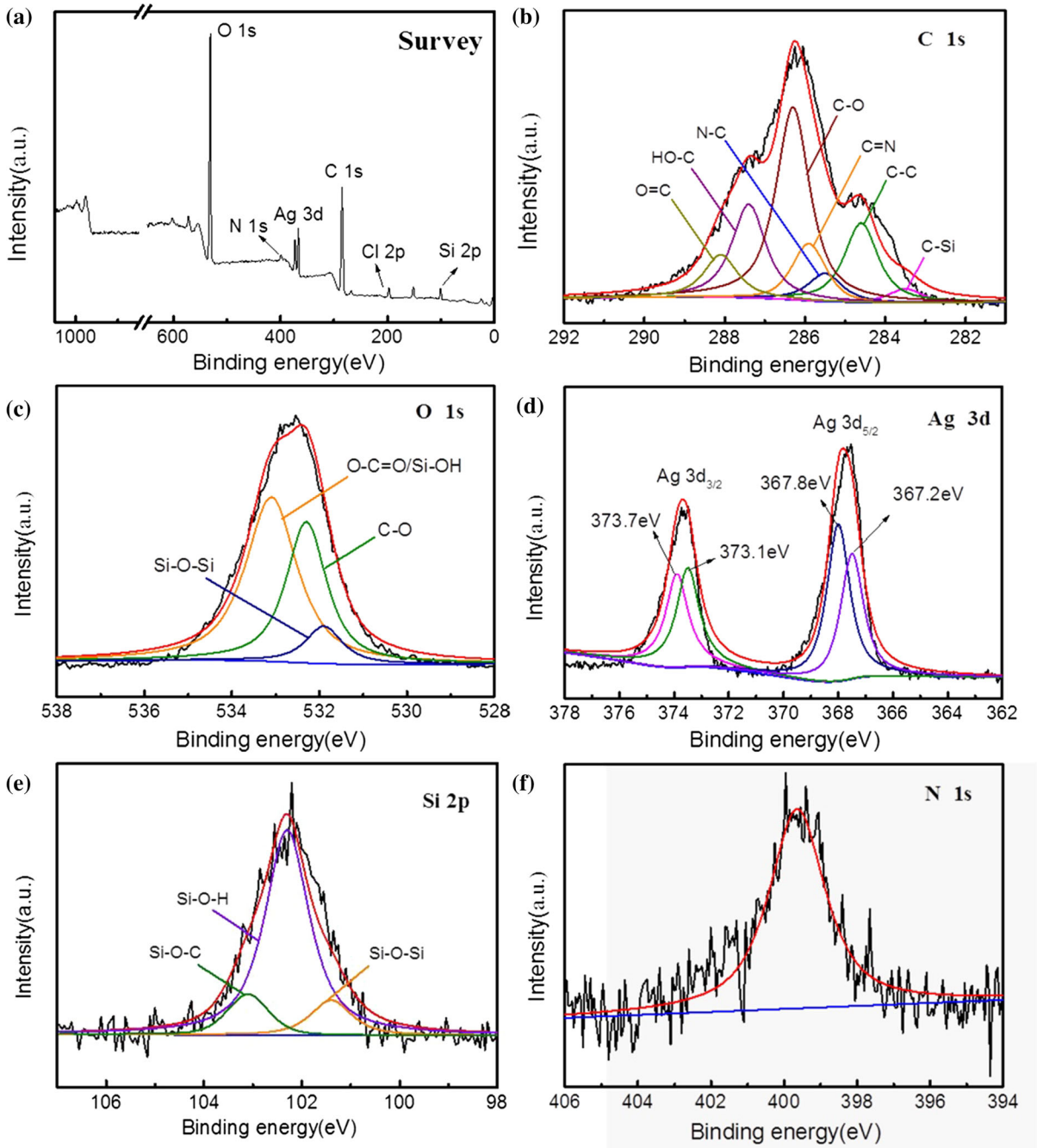

Fig. 3 XPS spectrum of **a** Ag/AgCl/CeO_2–CF and its high-resolution XPS spectra: **b** C 1s; **c** O 1s; **d** Ag 3d; **e** Si 2p; **f** N 1s

CeO_2–CF5 has high photocatalytic activity for different dyes. Meanwhile, the comparison optical images of the colors of dye solutions before and after degradation were inserted in Fig. 6c. The color of solutions all changed to colorless after visible light irradiation. Additionally, the degradation efficiency of Ag/AgCl/CeO_2–CF towards MB under nature sunlight irradiation was about 95.2% within 75 min irradiation (Fig. S4), indicating its bright prospect in practical application.

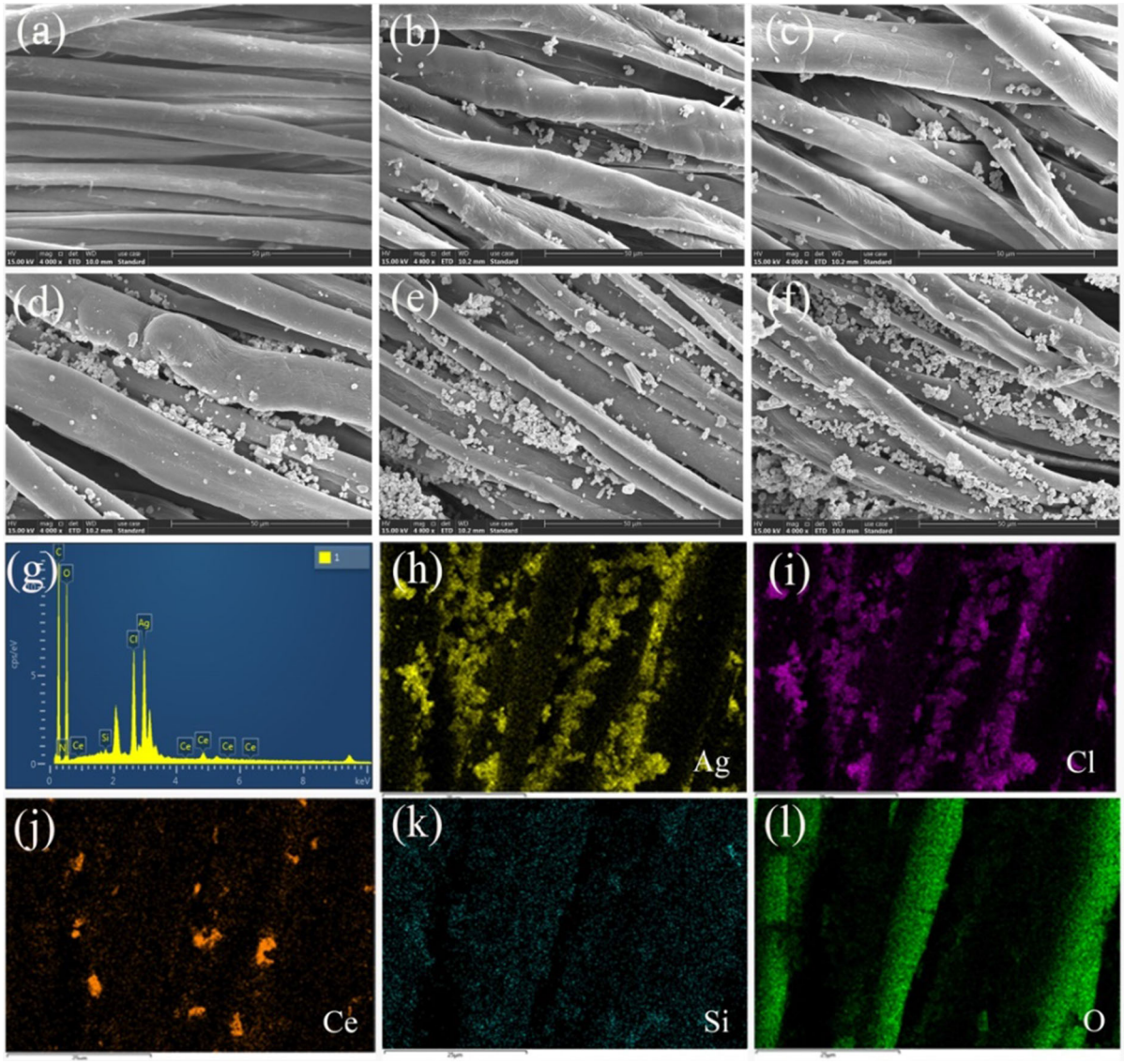

Fig. 4 SEM images of **a** CF; **b** Ag/AgCl/CeO_2–CF1; **c** Ag/AgCl/CeO_2–CF2; **d** Ag/AgCl/CeO_2–CF3; **e** Ag/AgCl/CeO_2–CF4; **f** Ag/AgCl/CeO_2–CF5; **g** EDS spectrum of Ag/AgCl/CeO_2–CF5; **h** Ag element map; **i** Cl element map; **j** Ce element map; **k** Si element map; **l** O element map, respectively

Photocatalytic stability of Ag/AgCl/CeO_2 decorated cotton fabrics

Apart from photocatalytic efficiency, reusability and stability of the prepared catalyst are also crucial parameters to assess its performance in practical application. The photocatalytic stability of Ag/AgCl/CeO_2–CF5 was investigated by recycle photodegradation of MB solution under visible-light irradiation. Herein, the photocatalytic stability of Ag/AgCl/CeO_2–CF0 was also investigated for comparison. As indicated in Fig. 7, the result reveals after five recycling runs for MB removal, the photocatalytic activity of Ag/AgCl/CeO_2–CF5 was not significantly decreased during the recycle experiments; its photocatalytic degradation efficiency was maintained at approximately 91.8% and around 80.7% after three and five cycles, respectively. However, as for Ag/

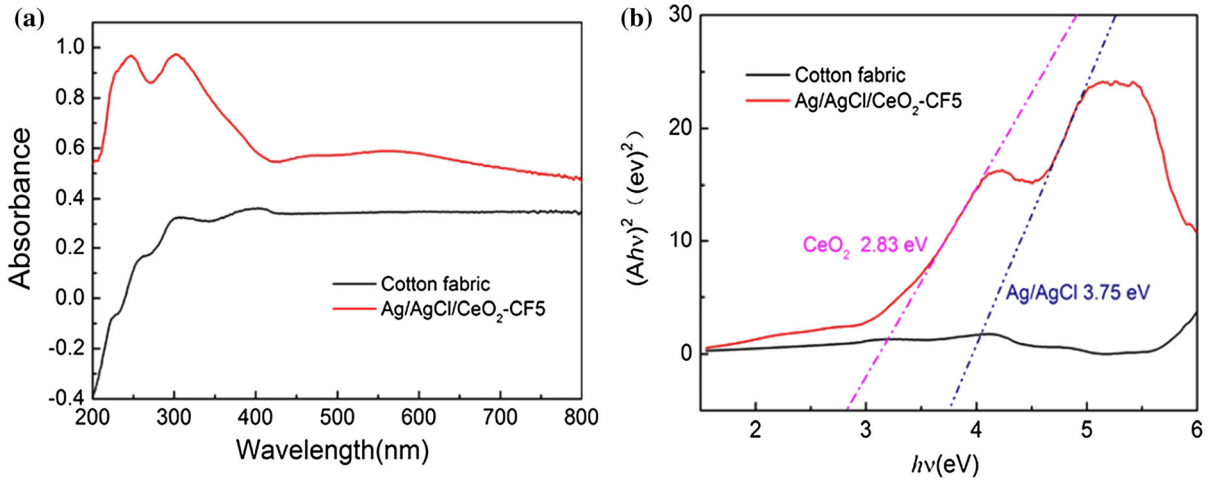

Fig. 5 UV–Vis diffuse reflectance spectra of **a** Ag/AgCl/CeO_2–CF5 and cotton fabric; **b** the curve between $(Ahv)^2$ and photon energy (hv) of the as-prepared samples

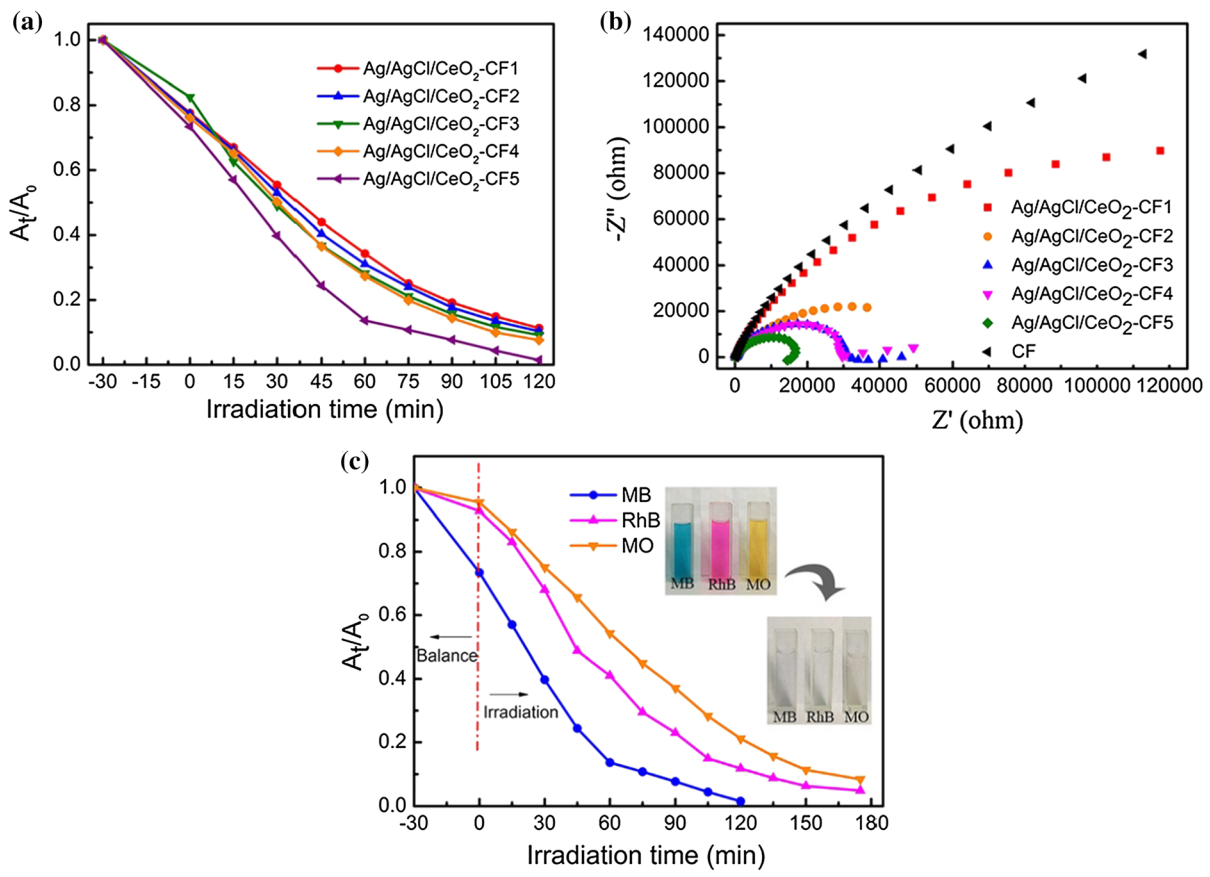

Fig. 6 **a** Photocatalytic degradation of MB by different samples under visible-light irradiation, **b** EIS spectra of different samples, **c** photocatalytic degradation of different dyes by Ag/AgCl/CeO_2–CF5 under visible-light irradiation

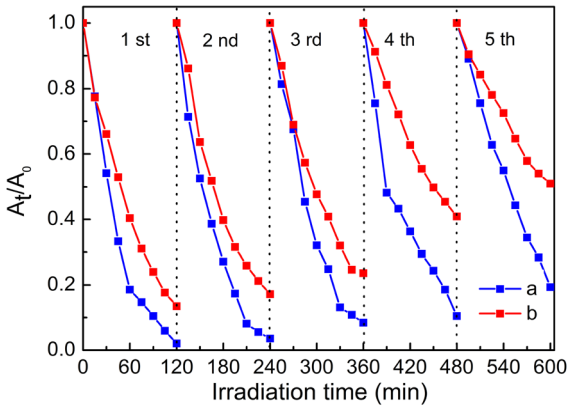

Fig. 7 Cycle of photodegradation of MB (MB = 20 mg L^{-1}; 50 mL) by **a** Ag/AgCl/CeO_2–CF5 and **b** Ag/AgCl/CeO_2–CF0, respectively

AgCl/CeO_2–CF0, the photocatalytic degradation efficiency sharply decreased from 86.6 to 49.1% after five cycles. This decrease might be attributed large amount of Ag/AgCl/CeO_2 detached from cotton fabric during the recycle processes. Therefore, the Ag/AgCl/CeO_2–CF5 composites had better photocatalytic stability than Ag/AgCl/CeO_2–CF0 in the photodegradation process. Importantly, the SEM image of Ag/AgCl/CeO_2–CF5 after five cycles clearly showed that its surface morphology was similar to the freshly prepared Ag/AgCl/CeO_2–CF5 (Fig. S5). It also confirmed that the Ag/AgCl/CeO_2 did not easily to fall off of the composite during the photocatalytic process. On the basis of above results, it indicates that Ag/AgCl/CeO_2–CF5 will be an effective photocatalyst in environmental remediation.

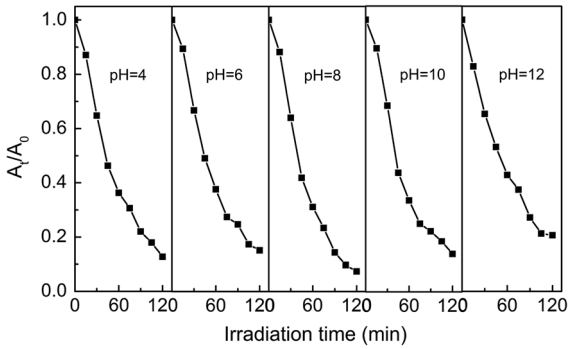

Fig. 8 Photocatalytic degradation of MB by Ag/AgCl/CeO_2–CF5 with pH values under visible-light irradiation

To be noted, the initial pH of the degradation solution is one of the influential parameters on the catalyst surface and oxidation power of free radicals; it might have a great effect on photocatalytic reactions. As shown in Fig. 8, a series of pH values were controlled by NaOH or CH_3COOH to explore the effect of the pH value of solution on the photocatalytic process. The photodegradation efficiency increased with increasing of pH from 4 to 8 and then decreased with further increase with pH value of solution. Therefore, the Ag/AgCl/CeO_2–CF5 displayed the best phtodegradation efficiency towards MB under neutral environment. The reasons can be explained as follows. Under the acidic solutions, the Ag/AgCl/CeO_2 surface presents positively charged in acidic medium, electrostatic interactions between the photocatalyst surface and MB (cationic dye) are weak, resulting in decrease adsorption (Li et al. 2015; Liu et al. 2015). Meanwhile, it is not conducive to the production of hydroxyl radicals under alkaline conditions, resulting in the decease of photocatalytic efficiency (Mohamed et al. 2017; Fan et al. 2018). Generally, Ag/AgCl/CeO_2–CF5 exhibited acceptable photocatalytic efficiency under broad pH range.

Mechanism of photocatalytic activity enhancement

In order to explore the predominant active species generated in the reaction system, three typical chemicals, t-BuOH, EDTA-2Na and *p*-benzoquinone (BQ) were employed as the scavengers of superoxide

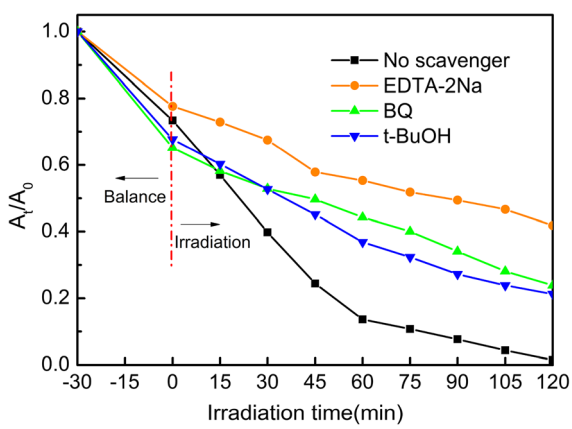

Fig. 9 Effects of various scavengers on the photocatalytic degradation of MB

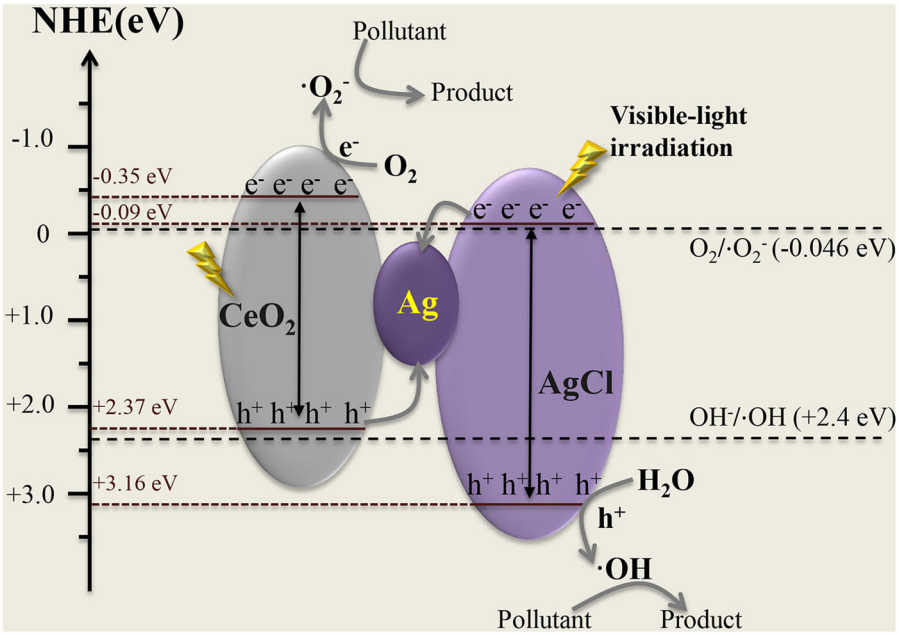

Scheme 2 Possible photocatalytic mechanism of MB with Ag/AgCl/CeO_2–CF

radical ($^{\cdot}OH$), hole (h^+) and hydroxyl radical ($^{\cdot}O_2^-$), respectively (Chen et al. 2016; Serpone et al. 2000; Zhao et al. 2012). As depicted in Fig. 9, the degradation efficiency of Ag/AgCl/CeO_2–CF without any scavengers can reach 99.5% within 120 min. When 1 mmol of t-BuOH and BQ as the scavenger for $^{\cdot}OH$ and $^{\cdot}O_2^-$ radical species was added into the photocatalytic procedure separately, the degradation efficiency of Ag/AgCl/CeO_2–CF decreased from 99.5 to 86.2% and 82.8%, and the degradation efficiency of Ag/AgCl/CeO_2–CF decreased to 59.2% in the presence of 1 mmol EDTA-2Na. Thus, it can be inferred that for MB photocatalytic degradation in the Ag/AgCl/CeO_2–CF composite system, $^{\cdot}OH$, h^+ and $^{\cdot}O_2^-$ all play a role in the whole photocatalytic reaction, but holes played important roles compared to $^{\cdot}OH$ and $^{\cdot}O_2^-$.

On the basis of the above results, a reasonable photocatalytic mechanism was proposed (Scheme 2). First of all, the valence band (Wen et al. 2017) (VB) of CeO_2 (+ 2.37 eV) is more negative than oxidation potential of $OH^-/^{\cdot}OH$ (+ 2.40 eV), meaning that the H_2O cannot be oxidized by photo excited holes in theory. Meanwhile, $^{\cdot}O_2^-$ is also cannot be generated in the AgCl because the conduction band (CB) of CeO_2 (− 0.353 eV) is more negative than AgCl (+ 0.09 eV) (Zhu et al. 2016; Li et al. 2018). Secondly, Ag nanoparticles were good electron acceptors with a lower Fermi level than the CB of AgCl, which promotes the transfer of photoelectrons from AgCl to Ag nanoparticles under visible light radiation, and then recombine with holes that transferred from the VB of CeO_2. As a result, the photoelectrons were effectively separated. Meanwhile, the electrons in the CB of CeO_2 can react with the O_2 to form reactive superoxide radicals. The holes at VB of AgCl can react with H_2O molecules to form $^{\cdot}OH$ or oxidize Cl^- to Cl^0. Subsequently, the formed h^+, $^{\cdot}OH$, Cl^0 and $^{\cdot}O_2^-$ were taken part in the MB photodegradation system. This analysis was identical with the results of trapping experiment of reactive species.

Conclusion

To sum up, novel Ag/AgCl/CeO_2 decorated cotton fabrics were successfully fabricated via "amine–aldehyde" chemistry. Interestingly, the amount of Ag/AgCl/CeO_2 on the cotton fabric surface can be adjusted by the degree of aldehyde of cotton fabrics. As results, the Ag/AgCl/CeO_2–CFs presented excellent photocatalytic activity towards synthetic dyes.

The degradation efficiencies of Ag/AgCl/CeO_2–CFs for MB, RhB and MO can all reach approximately 95% within 180 min under visible light irradiation. Meanwhile, the Ag/AgCl/CeO_2–CFs presented good stability under various acidic and basic solutions, the degradation efficiency could maintain above 80.0% after five degradation cycles. Most importantly, the Ag/AgCl/CeO_2–CFs can be easily reused without centrifugation and filtration. Therefore, it is proposed that Ag/AgCl/CeO_2–CFs could be a promising candidate for the removal of various dyes from industrial waste for environmental remediation.

Acknowledgments This work was supported by the Fundamental Research Funds for the Central Universities (No. YJ201823) and Sichuan Science and Technology Program (2020YJ0316). We would like to thank the Analytical & Testing Center of Sichuan University for SEM and XPS measurements. We also thank Sha Deng and Mi Zhou for the experimental assistance.

References

Bi Y, Ye J (2009) In situ oxidation synthesis of Ag/AgCl core–shell nanowires and their photocatalytic properties. Chem Commun (Camb) 43:6551–6553. https://doi.org/10.1039/b913725d

Chen F, Yang Q, Niu C, Li X, Zhang C, Zhao J, Xu Q, Zhong Y, Deng Y, Zeng G (2016) Enhanced visible light photocatalytic activity and mechanism of $ZnSn(OH)_6$ nanocubes modified with AgI nanoparticles. Catal Commun 73:1–6. https://doi.org/10.1016/j.catcom.2015.10.003

Chen Y, Zhou L, Chen L, Duan G, Mei C, Huang C, Han J, Jiang S (2019) Anisotropic nanocellulose aerogels with ordered structures fabricated by directional freeze-drying for fast liquid transport. Cellulose 26:6653–6667. https://doi.org/10.1007/s10570-019-02557-z

Cheng M, Zeng G, Huang D, Lai C, Xu P, Zhang C, Liu Y, Wan J, Gong X, Zhu Y (2016) Degradation of atrazine by a novel Fenton-like process and assessment the influence on the treated soil. J Hazard Mater 312:184–191. https://doi.org/10.1016/j.jhazmat.2016.03.033

Dong X, Cui W, Wang H, Li J, Sun Y, Wang H, Zhang Y, Huang H, Dong F (2019) Promoting ring-opening efficiency for suppressing toxic intermediates during photocatalytic toluene degradation via surface oxygen vacancies. Sci Bull 64:669–678. https://doi.org/10.1016/j.scib.2019.04.020

Du Z, Cheng C, Tan L, Lan J, Jiang S, Zhao L, Guo R (2018) Enhanced photocatalytic activity of Bi_2WO_6/TiO_2 composite coated polyester fabric under visible light irradiation. Appl Surf Sci 435:626–634. https://doi.org/10.1016/j.scib.2019.04.020

Fan G, Luo J, Guo L, Lin R, Zheng X, Snyder SA (2018) Doping Ag/AgCl in zeolitic imidazolate framework-8 (ZIF-8) to enhance the performance of photodegradation of methylene blue. Chemosphere 209:44–52. https://doi.org/10.1016/j.apsusc.2017.11.136

Fu MC, Shang R, Zhao B, Wang B, Fu Y (2019) Photocatalytic decarboxylative alkylations mediated by triphenylphosphine and sodium iodide. Science 363:1429–1434. https://doi.org/10.1016/j.chemosphere.2018.06.036

Gashti MP, Alimohammadi F, Shamei A (2012) Preparation of water-repellent cellulose fibers using a polycarboxylic acid/hydrophobic silica nanocomposite coating. Surf Coat Technol 206:3208–3215. https://doi.org/10.1016/j.surfcoat.2012.01.006

Guan X, Lin S, Lan J, Shang J, Li W, Zhan Y, Xiao H, Song Q (2019) Fabrication of Ag/AgCl/ZIF-8/TiO_2 decorated cotton fabric as a highly efficient photocatalyst for degradation of organic dyes under visible light. Cellulose 26:7437–7450. https://doi.org/10.1007/s10570-019-02621-8

He J, Shao DW, Zheng LJ, Zheng RK, Zheng LC, Feng DQ, Xu JP, Zhang XH, Wang WC, Wang WH, Lu F, Dong H, Cheng YH, Liu H (2017) Construction of Z-scheme Cu_2O/Cu/AgBr/Ag photocatalyst with enhanced photocatalytic activity and stability under visible light. Appl Catal B Environ 203:917–926. https://doi.org/10.1016/j.apcatb.2016.10.086

Jiang J, Zhang L (2011) Rapid microwave-assisted nonaqueous synthesis and growth mechanism of AgCl/Ag, and its daylight-driven plasmonic photocatalysis. Chemistry 17:3710–3717. https://doi.org/10.1002/chem.201002951

Jiang X, Lai S, Xu W, Fang J, Chen X, Beiyuan J, Zhou X, Lin K, Liu J, Guan G (2019) Novel ternary BiOI/g-C_3N_4/CeO_2 catalysts for enhanced photocatalytic degradation of tetracycline under visible-light radiation via double charge transfer process. J Alloys Compd 809:151804. https://doi.org/10.1016/j.jallcom.2019.151804

Kaviyarasu K, Manikandan E, Kennedy J, Maaza M (2016) Synthesis and analytical applications of photoluminescent carbon nanosheet by exfoliation of graphite oxide without purification. J Mater Sci Mater Electron 27:13080–13085. https://doi.org/10.1007/s10854-016-5451-z

Li H, Wang R, Hu H, Liu W (2008) Surface modification of self-healing poly(urea-formaldehyde) microcapsules using silane-coupling agent. Appl Surf Sci 255:1894–1900. https://doi.org/10.1016/j.apsusc.2008.06.170

Li B, Wu L, Li L, Seeger S, Zhang J, Wang A (2014) Superwetting double-layer polyester materials for effective removal of both insoluble oils and soluble dyes in water. ACS Appl Mater Interfaces 6:11581–11588. https://doi.org/10.1021/am502313h

Li W, Ma Z, Bai G, Hu J, Guo X, Dai B, Jia X (2015) Dopamine-assisted one-step fabrication of Ag@AgCl nanophotocatalyst with tunable morphology, composition and improved photocatalytic performance. Appl Catal B Environ 174–175:43–48. https://doi.org/10.1016/j.apcatb.2015.02.029

Li B, Lai C, Zeng G, Qin L, Yi H, Huang D, Zhou C, Liu X, Cheng M, Xu P, Zhang C, Huang F, Liu S (2018) Facile hydrothermal synthesis of Z-scheme $Bi_2Fe_4O_9/Bi_2WO_6$ heterojunction photocatalyst with enhanced visible light photocatalytic activity. ACS Appl Mater Interfaces 10:18824–18836. https://doi.org/10.1021/acsami.8b06128

Li C, Wang J, Luo Y, Wang F, Zhu H, Guo Y (2019a) One-bath two step method combined surface micro/nanostructures treatment to enhance antifouling and antibacterial property of PTFE flat membrane. J Taiwan Inst Chem Eng 96:639–651. https://doi.org/10.1016/j.jtice.2019a.01.001

Li J, Dong X, Zhang G, Cui W, Cen W, Wu Z, Lee SC, Dong F (2019b) Probing ring-opening pathways for efficient photocatalytic toluene decomposition. J Mater Chem A 7:3366–3374. https://doi.org/10.1039/C8TA11627J

Lin W, Zhang S, Wang D, Zhang C, Sun D (2015) Ultrasound-assisted synthesis of high-efficiency Ag_3PO_4/CeO_2 heterojunction photocatalyst. Ceram Int 41:8956–8963. https://doi.org/10.1016/j.ceramint.2015.03.169

Liu X, Yang Y, Shi X, Li K (2015) Fast photocatalytic degradation of methylene blue dye using a low-power diode laser. J Hazard Mater 283:267–275. https://doi.org/10.1016/j.jhazmat.2014.09.031

Liu J, Li R, Hu Y, Li T, Jia Z, Wang Y, Wang Y, Zhang X, Fan C (2017) Harnessing Ag nanofilm as an electrons transfer mediator for enhanced visible light photocatalytic performance of Ag@AgCl/Ag nanofilm/ZIF-8 photocatalyst. Appl Catal B Environ 202:64–71. https://doi.org/10.1016/j.apcatb.2016.09.015

Mohamed A, Yousef S, Ali Abdelnaby M, Osman TA, Hamawandi B, Toprak MS, Muhammed M, Uheida A (2017) Photocatalytic degradation of organic dyes and enhanced mechanical properties of PAN/CNTs composite nanofibers. Sep Purif Technol 182:219–223. https://doi.org/10.1016/j.seppur.2017.03.051

Montazer M, Pakdel E (2011) Functionality of nano titanium dioxide on textiles with future aspects: focus on wool. J Photochem Photobiol C Photochem Rev 12:293–303. https://doi.org/10.1016/j.jphotochemrev.2011.08.005

Monti S, Pastore M, Li C, De Angelis F, Carravetta V, Teoretisk KOB, Skolan FBB (2016) Theoretical investigation of adsorption, dynamics, self-aggregation, and spectroscopic properties of the D102 indoline dye on an anatase (101) substrate. J Phys Chem C 120:2787–2796. https://doi.org/10.1021/acs.jpcc.5b11332

Ouyang W, Liu S, Yao K, Zhao L, Cao L, Jiang S, Hou H (2018) Ultrafine hollow TiO_2 nanofibers from core–shell composite fibers and their photocatalytic properties. Compos Commun 9:76–80. https://doi.org/10.1016/j.coco.2018.06.006

Peng X, Hu F, Zhang T, Qiu F, Dai H (2018) Amine-functionalized magnetic bamboo-based activated carbon adsorptive removal of ciprofloxacin and norfloxacin: a batch and fixed-bed column study. Biores Technol 249:924–934. https://doi.org/10.1016/j.biortech.2017.10.095

Qi Y, Ye J, Zhang S, Tian Q, Xu N, Tian P, Ning G (2019) Controllable synthesis of transition metal ion-doped CeO_2 micro/nanostructures for improving photocatalytic performance. J Alloys Compd 782:780–788. https://doi.org/10.1016/j.jallcom.2018.12.111

Qin Q, Guo R, Lin S, Jiang S, Lan J, Lai X, Cui C, Xiao H, Zhang Y (2019) Waste cotton fiber/Bi_2WO_6 composite film for dye removal. Cellulose 26:3909–3922. https://doi.org/10.1007/s10570-019-02345-9

Rafatullah M, Sulaiman O, Hashim R, Ahmad A (2010) Adsorption of methylene blue on low-cost adsorbents: a review. J Hazard Mater 177:70–80. https://doi.org/10.1016/j.jhazmat.2009.12.047

Ran J, Bi S, Jiang H, Telegin F, Bai X, Yang H, Cheng D, Cai G, Wang X (2019) Core–shell $BiVO_4$@PDA composite photocatalysts on cotton fabrics for highly efficient photodegradation under visible light. Cellulose 26:6259–6273. https://doi.org/10.1007/s10570-019-02535-5

Sangsefidi FS, Salavati-Niasari M, Khojasteh H, Shabani-Nooshabadi M (2017) Synthesis, characterization and investigation of the electrochemical hydrogen storage properties of CuO–CeO_2 nanocomposites synthesized by green method. Int J Hydrog Energy 42:14608–14620. https://doi.org/10.1016/j.ijhydene.2017.04.103

Serpone N, Texier I, Emeline AV, Pichat P, Hidaka H, Zhao J (2000) Post-irradiation effect and reductive dechlorination of chlorophenols at oxygen-free TiO_2/water interfaces in the presence of prominent hole scavengers. J Photochem Photobiol A Chem 136:145–155. https://doi.org/10.1016/S1010-6030(00)00348-8

Shekofteh-Gohari M, Habibi-Yangjeh A, Abitorabi M, Rouhi A (2018) Magnetically separable nanocomposites based on ZnO and their applications in photocatalytic processes: a review. Crit Rev Environ Sci Technol 48:806–857. https://doi.org/10.1080/10643389.2018.1487227

Sun C, Wu Y, Zhang W, Jiang N, Jiu T, Fang J (2014) Improving efficiency by hybrid TiO_2 nanorods with 1,10-phenanthroline as a cathode buffer layer for inverted organic solar cells. ACS Appl Mater Interfaces 6:739–744. https://doi.org/10.1021/am404423k

Tauc JC (1974) Amorphous and liquid semiconductors. Springer, Boston, pp 25–27

Tissera ND, Wijesena RN, Perera JR, de Silva KMN, Amaratunge GAJ (2015) Hydrophobic cotton textile surfaces using an amphiphilic graphene oxide (GO) coating. Appl Surf Sci 324:455–463. https://doi.org/10.1016/j.apsusc.2014.10.148

Wan X, Zhan Y, Long Z, Zeng G, Ren Y, He Y (2017) High-performance magnetic poly(arylene ether nitrile) nanocomposites: co-modification of Fe_3O_4 via mussel inspired poly(dopamine) and amino functionalized silane KH550. Appl Surf Sci 425:905–914. https://doi.org/10.1016/j.apsusc.2017.07.136

Wang Y, Ding X, Chen X, Chen Z, Zheng K, Chen L, Ding J, Tian X, Zhang X (2017) Layer-by-layer self-assembly photocatalytic nanocoating on cotton fabrics as easily recycled photocatalyst for degrading gas and liquid pollutants. Cellulose 24:4569–4580. https://doi.org/10.1016/j.apsusc.2017.07.136

Wen X, Niu C, Huang D, Zhang L, Liang C, Zeng G (2017) Study of the photocatalytic degradation pathway of norfloxacin and mineralization activity using a novel ternary Ag/AgCl–CeO_2 photocatalyst. J Catal 355:73–86. https://doi.org/10.1016/j.jcat.2017.08.028

Wen Z, Xu C, Qian X, Zhang Y, Zhang C, Wang X, Song S, Dai M (2019) A two-step carbon fiber surface treatment and its effect on the interfacial properties of CF/EP composites: the electrochemical oxidation followed by grafting of silane coupling agent. Appl Surf Sci 486:546–554. https://doi.org/10.1016/j.jcat.2017.11.029

Wu X, Cai J, Li S, Zheng F, Lai Z, Zhu L, Chen T (2016) Au@Cu_2O stellated polytope with core–shelled

nanostructure for high-performance adsorption and visible-light-driven photodegradation of cationic and anionic dyes. J Colloid Interface Sci 469:138–146. https://doi.org/10.1016/j.jcis.2016.01.064

Yadav VSK, Purkait MK (2016) Simultaneous CO_2 reduction and dye (crystal violet) removal electrochemically on Sn and Zn electrocatalysts using Co_3O_4 anode. Energy Fuels 30:3340–3346. https://doi.org/10.1021/acs.energyfuels.6b00047

Yang Z, Tarabara VV, Bruening ML (2015) Adsorption of anionic or cationic surfactants in polyanionic brushes and its effect on brush swelling and fouling resistance during emulsion filtration. Langmuir 31:11790–11799. https://doi.org/10.1021/acs.langmuir.5b01938

Yao X, Liu X (2014) One-pot synthesis of ternary Ag_2CO_3/Ag/AgCl photocatalyst in natural geothermal water with enhanced photocatalytic activity under visible light irradiation. J Hazard Mater 280:260–268. https://doi.org/10.1016/j.jhazmat.2014.07.079

Yi H, Yan M, Huang D, Zeng G, Lai C, Li M, Li B, Huo X, Qin L, Liu S, Liu X, Wang H, Shen M, Fu Y, Guo X (2019) Synergistic effect of artificial enzyme and 2D nano-structured Bi_2WO_6 for eco-friendly and efficient biomimetic photocatalysis. Appl Catal B Environ 250:52–62. https://doi.org/10.1016/j.apcatb.2019.03.008

Yu D, Bai J, Liang H, Ma T, Li C (2016) AgI-modified TiO_2 supported by PAN nanofibers: a heterostructured composite with enhanced visible-light catalytic activity in degrading MO. Dyes Pigm 133:51–59. https://doi.org/10.1016/j.dyepig.2016.05.036

Zang Y, Farnood R (2008) Photocatalytic activity of AgBr/TiO_2 in water under simulated sunlight irradiation. Appl Catal B Environ 79:334–340. https://doi.org/10.1016/j.apcatb.2007.10.019

Zhan Y, Guan X, Ren E, Lin S, Lan J (2019) Fabrication of zeolitic imidazolate framework-8 functional polyacrylonitrile nanofibrous mats for dye removal. J Polym Res 26:145. https://doi.org/10.1007/s10965-019-1806-5

Zhang S, Li J, Wang X, Huang Y, Zeng M, Xu J (2014) In situ ion exchange synthesis of strongly coupled Ag@AgCl/g-C_3N_4 porous nanosheets as plasmonic photocatalyst for highly efficient visible-light photocatalysis. ACS Appl Mater Interfaces 6:22116–22125. https://doi.org/10.1021/am505528c

Zhao Y, Eley C, Hu J, Foord JS, Ye L, He H, Tsang SC (2012) Shape-dependent acidity and photocatalytic activity of Nb_2O_5 nanocrystals with an active TT (001) surface. Angew Chem Int Ed Engl 51:3846–3849. https://doi.org/10.1002/anie.201108580

Zhao J, Lu C, He X, Zhang X, Zhang W, Zhang X (2015) Polyethylenimine-grafted cellulose nanofibril aerogels as versatile vehicles for drug delivery. ACS Appl Mater Interfaces 7:2607–2615. https://doi.org/10.1021/am507601m

Zhu W, Liu L, Liao Q, Chen X, Qian Z, Shen J, Liang J, Yao J (2016) Functionalization of cellulose with hyperbranched polyethylenimine for selective dye adsorption and separation. Cellulose 23:3785–3797. https://doi.org/10.1007/s10570-016-1045-4

Zinatloo-Ajabshir S, Salavati-Niasari M (2016) Facile route to synthesize zirconium dioxide (ZrO_2) nanostructures: structural, optical and photocatalytic studies. J Mol Liq 216:545–551. https://doi.org/10.1016/j.molliq.2016.01.062